Journal of Magnetic Resonance 308 (2019) 106559

Contents lists available at ScienceDirect

Journal of Magnetic Resonance

journal homepage: www.elsevier.com/locate/jmr

Accurate ^{1}H-^{14}N distance measurements by phase-modulated RESPDOR at ultra-fast MAS

Nghia Tuan Duong [a], Federica Rossi [b], Maria Makrinich [c], Amir Goldbourt [c], Michele R. Chierotti [b], Roberto Gobetto [b], Yusuke Nishiyama [a,d,*]

[a] NMR Science and Development Division, RIKEN SPring-8 Center, and Nano-Crystallography Unit, RIKEN-JEOL Collaboration Center, Yokohama, Kanagawa 230-0045, Japan
[b] Department of Chemistry and NIS Centre, University of Torino, V.P. Giuria 7, 10125, Italy
[c] School of Chemistry, Raymond and Beverly Sackler Faculty of Exact Sciences, Tel Aviv University, Ramat Aviv, Tel Aviv 6997801, Israel
[d] JEOL RESONANCE Inc., Musashino, Akishima, Tokyo 196-8558, Japan

ARTICLE INFO

Article history:
Received 8 May 2019
Revised 12 July 2019
Accepted 12 July 2019
Available online 13 July 2019

Keywords:
^{1}H-^{14}N distance measurement
Phase-modulated pulse
S-RESPDOR
Ultra-fast MAS

ABSTRACT

The combination of a phase-modulated (PM) saturation pulse and symmetry-based dipolar recoupling into a rotational-echo saturation-pulse double-resonance (RESPDOR) sequence has been employed to measure ^{1}H-^{14}N distances. Such a measurement is challenging owing to the quadrupolar interaction of ^{14}N nucleus and the intense ^{1}H-^{1}H homonuclear dipolar interactions. Thanks to the recent advances in probe technology, the homonuclear dipolar interaction can be sufficiently suppressed at a fast MAS frequency ($\nu_R \geq 60$ kHz). PM pulse is robust to large variations of parameters on quadrupolar spins, but it has not been demonstrated under very fast MAS conditions. On the other hand, the RESPDOR sequence is applicable to such condition when it employs symmetry-based pulses during the recoupling period, but a prior knowledge on the system is required. In this article, we demonstrated the PM-RESPDOR combination for providing accurate ^{1}H-^{14}N distances at a very fast MAS frequency of 70 kHz on two samples, namely L-tyrosine·HCl and N-acetyl-L-alanine. This sequence, supported by simulations and experiments, has shown its feasibility at $\nu_R = 70$ kHz as well as the robustness to the ^{14}N quadrupolar interaction. It is applicable to a wide range of ^{1}H-^{14}N dipolar coupling constants when a radio frequency field on the ^{14}N channel is approximately 80 kHz or more, while the PM pulse length lasts 10 rotor periods. For the first time, multiple ^{1}H-^{14}N heteronuclear dipolar couplings, thus multiple quantitative distances, are simultaneously and reliably extracted by fitting the experimental fraction curves with the analytical expression. The size of the ^{1}H-^{14}N dipolar interaction is solely used as a fitting parameter. These determined distances are in excellent agreement with those derived from diffraction techniques.

© 2019 Elsevier Inc. All rights reserved.

1. Introduction

The accurate measurement of H-N distances is of importance in chemistry, biology, and pharmacy. Such distances can be used as structural restraints for three-dimensional structural refinements of peptides and proteins [1,2], or they can be served for unambiguous distinction of cocrystals/salts drugs [3], to name a few. Traditionally, X-ray and neutron diffraction techniques have been preferred for extracting those distances; however, while X-ray analysis has the difficulty in precise determination of ^{1}H positions, the neutron-based method requires large scale facilities and sufficiently large crystals and/or deuteration, which are difficult to achieve for many samples. Solid-state nuclear magnetic resonance (ssNMR) has long been utilized as the complementary method for structure refinement since it (i) enables the measurements with no restriction of sample morphologies (microcrystalline, disordered or amorphous states), and (ii) directly provides distances between two atoms via their dipolar coupling, which is inversely proportional to the cube of the internuclear distance. The capability and versatility of ssNMR in extracting structural information is greatly enhanced by the combination of magic-angle spinning (MAS) [4] and recoupling sequences [5,6]. Under the MAS condition, high-resolution spectra are achieved due to the suppression of anisotropic interactions such as homo-/heteronuclear dipolar couplings and chemical shift anisotropy (CSA), leading to the loss of structural information. To avoid such losses, the suppressed anisotropic interactions can be selectively recovered by recoupling sequences. It is worth noting that for accurate quantification of ^{1}H-N dipolar interactions, the ^{1}H-N recoupling technique is also required to

* Corresponding author at: NMR Science and Development Division, RIKEN SPring-8 Center, and Nano-Crystallography Unit, RIKEN-JEOL Collaboration Center, Yokohama, Kanagawa 230-0045, Japan.
E-mail address: yunishiy@jeol.co.jp (Y. Nishiyama).

https://doi.org/10.1016/j.jmr.2019.07.046
1090-7807/© 2019 Elsevier Inc. All rights reserved.

suppress the intense ^{1}H-^{1}H homonuclear dipolar couplings. A number of methods have been developed to meet this additional requirement [7–12], among which R-symmetry approach is the most promising owing to the ease in designing sequences at various experimental conditions [13–17]. For example, Polenova and coworkers have introduced the phase-alternating R-type symmetry (PARS) sequence to yield ^{1}H-^{13}C and ^{1}H-^{15}N distances for a variety of samples, even fully protonated systems at moderate and fast MAS frequencies (up to 40 kHz) [16]. However, the disadvantages of this sequence are the requirement of high radio frequency (rf) on the ^{1}H channel (at least 2.5 times larger than the MAS frequency) as well as its sensitivity to rf imperfections and/or inhomogeneity. Its later development, the windowed PARS sequence, has overcome the sensitivity issue, but even higher rf-field is required [17].

Contemporary advances in fast MAS probe technology have opened possibilities for new experimental designs. Under very fast MAS frequency, the ^{1}H-^{1}H homonuclear dipolar interactions are sufficiently suppressed, simplifying the use of ^{1}H-N recoupling sequences. Moreover, thanks to such suppression, highly resolved proton spectra can be achieved, allowing proton detection, thus providing significant enhancement in sensitivity. Several cross-polarization (CP)-based experiments and their proton-detected versions have been proposed at very fast MAS frequency ($\nu_R \geq 60$ kHz) for a simple and accurate determination of ^{1}H-^{15}N dipolar couplings [18,19]. Nevertheless, a major drawback of these methods is the low natural abundance of the ^{15}N isotope (0.4%). Even with proton-detected versions, sufficient signal intensity is only achieved by either isotopic labeling or long experimental time. On the other hand, the ^{14}N isotope benefits from a much higher natural abundance (99.6%); however, it is an integer quadrupolar nucleus (spin number $I = 1$), thus ^{14}N excitation schemes suffer from the large quadrupolar interactions and the lack of a central transition. Another difficulty with the ^{14}N nucleus is that while the applied rf field ($\nu_1(^{14}\mathrm{N})$) is in the range of tens of kHz due to its low Larmor frequency, the ^{14}N quadrupolar coupling constant (C_Q) is commonly in the range of MHz. These issues make ^{1}H-^{14}N distance measurement challenging. Although the ^{1}H-^{14}N distance measurements has been reported, such measurements required the prior knowledge on the ^{14}N quadrupolar interactions, the principal axes of ^{14}N electric field gradient tensors, and the scaling factor of the multiple pulse scheme [20].

In this article, we demonstrate ^{1}H-^{14}N distance measurements by using the rotational-echo saturation-pulse double-resonance (RESPDOR) technique. This sequence has been selected because (i) it is compatible with a high MAS frequency, which is mandatory for ^{1}H-detected experiments, (ii) it only requires moderate rf field strength on ^{14}N for efficient saturation of quadrupolar nuclei, and (iii) its fraction curve can be represented by an analytical curve in case of ideal saturation. The RESPDOR sequence was firstly introduced by Gan for ^{13}C-^{14}N distance measurements [21]. For this initial version, the recoupling of spatially close ^{13}C-^{14}N pairs was done by applying two rotary recoupling resonance (R^3) sequence blocks separated by a long continuous-wave pulse applied to the ^{14}N channel [22]. Later R^3 was replaced by the $SR4_1^2$ sequence [23]. The incorporation of $SR4_1^2$ into RESPDOR (S-RESPDOR) has extended the applications to various systems [24–27]. This is because $SR4_1^2$ is more robust with respect to CSA and rf inhomogeneity than R^3, and more importantly it allows the measurements of multiple distances due to the avoidance of dipolar truncation effects. However, the efficiency of RESPDOR still largely depends on C_Q and ν_1 since the extents of saturation of crystallites are different from each other. Such orientation-dependence effect requires the scaling of RESPDOR fraction curves in addition to the dipolar coupling adjustments in the fitting procedure, introducing ambiguity of distance measurements by S-RESPDOR. For extending the applicability of S-RESPDOR, a saturating pulse on the quadrupolar channel that weakly depends on the nature of a ^{1}H-^{14}N system is highly desired. Goldbourt and coworkers have introduced an elegant phase-modulated (PM) scheme into the original rotational-echo double-resonance (REDOR) sequence [28], allowing a uniform saturation for the entire powder crystallites even in the presence of large quadrupolar interactions using a moderate rf-field strength [29–32]. The PM pulse is also robust with respect to offset, and rf inhomogeneity [29,30]. These advances, of combining REDOR and the PM scheme (i.e. PM-RESPDOR), lead to a simple fitting procedure at moderate MAS frequencies, where only a single parameter, the dipolar coupling, is adjusted for matching the theoretical/simulated fraction curves with the experimental ones. However, a PM-S-RESPDOR sequence, which combines the $SR4_1^2$ symmetry-based recoupling element with the PM pulse has not yet been demonstrated, and has not been performed under fast MAS condition, which is the main aim of our present work. Herein, we demonstrate for the first time the ^{1}H-^{14}N distance measurements using PM-S-RESPDOR under $\nu_R = 70$ kHz. Firstly, by simulations, we examine the feasibility of PM-S-RESPDOR at a very fast MAS condition, and then investigate the effect of quadrupolar coupling and heteronuclear dipolar interaction on the fraction curves. Finally, the performance of this sequence is tested on the two model samples L-tyrosine·HCl and N-acetyl-L-alanine, and the distances obtained by fitting with the analytical expression are compared with those derived from diffraction techniques.

2. Pulse sequences

Fig. 1a shows the dipolar-heteronuclear multiple quantum coherence (*D*-HMQC) sequence for a two-dimensional (2D) ^{1}H-^{14}N correlation experiment [33–36]. Fig. 1b shows the PM-S-RESPDOR sequence for ^{1}H-^{14}N distance measurements. The designs of the two sequences are similar except for the use of a single PM pulse for saturation in PM-S-RESPDOR instead of a pair of pulses for single-quantum (SQ) excitation and reconversion

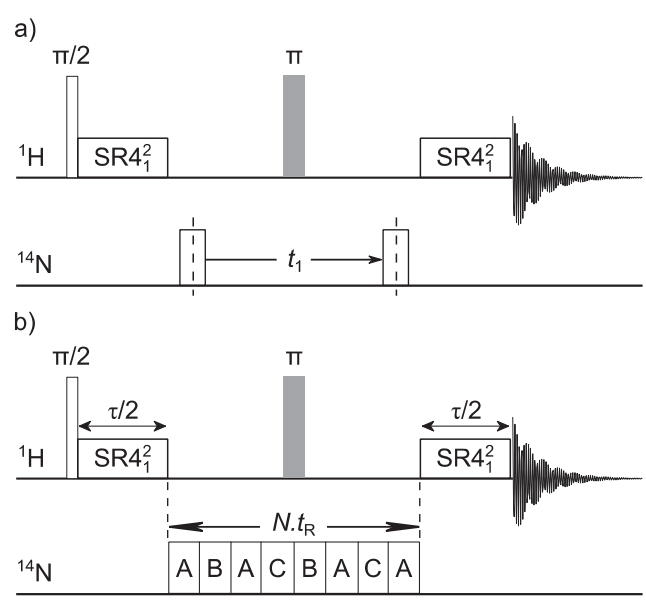

Fig. 1. (a) *D*-HMQC sequence. The 2D ^{1}H-^{14}N correlation spectrum was acquired by incrementing t_1. (b) PM-S-RESPDOR sequence. The fraction curve is obtained by incrementing the total mixing time (τ) of the $SR4_1^2$ blocks under the absence and presence of irradiation on ^{14}N channel. The PM pulse is the combination of A-B-A-C-B-A-C-A blocks. The pulse length of the PM pulse is $N{\cdot}t_R$, where N is an integer and t_R is the length of the rotor period. As the $SR4_1^2$ recoupling sequence is non-γ-encoded, the interval between these two blocks should be kept rotor-synchronized for both *D*-HMQC and PM-S-RESPDOR sequences.

during t_1 period in *D*-HMQC. The PM pulse, lasting for $N{\cdot}t_R$, is composed by the combination of A-B-A-C-B-A-C-A blocks. Block A consists of 1 (one) pulse, lasting for 0.075 * $N{\cdot}t_R$ and a phase of $\varphi_0 = 225$. Block B consists of 16 (sixteen) pulses. Each lasts for 0.0109375 * $N{\cdot}t_R$ with a phase of $\varphi_{i=1\text{-}16}$ = {80.5, 2.2, 245.0, 92.5, 275.7, 98.5, 330.3, 348.1, 126.3, 265.2, 349.3, 23.9, 24.1, 23.8, 92.4, 6.7}. Block C consists of 16 (sixteen) pulses. Each lasts for 0.0109375 * $N{\cdot}t_R$ with a phase of $\varphi_{i=1\text{-}16}$ = {319.6, 75.6, 242.7, 95.8, 340.9, 226.5, 48.0, 38.1, 5.3, 44.4, 145.8, 303.2, 139.7, 336.7, 95.6, 341.3}. The $SR4_1^2$ recoupling sequence was used to reintroduce the ^{1}H-^{14}N dipolar couplings. Since it is non-γ-encoded [37], the interval between the two $SR4_1^2$ blocks needs to be rotor-synchronized.

Two sets of data are recorded to extract distance information using the PM-S-RESPDOR sequence. Firstly, the experiment is run without irradiation of the PM pulse on the ^{14}N channel ($\nu_1(^{14}\text{N})$ = 0) during a delay of $N{\cdot}t_R$. Here, the ^{1}H-^{14}N heteronuclear dipolar coupling and ^{1}H CSA are refocused by the π pulse on the ^{1}H channel. It is noted that the ^{1}H-^{1}H homonuclear dipolar coupling is averaged by the use of $SR4_1^2$ sequence and MAS to the first-order. Consequently, the decaying of ^{1}H signals is due to the higher-order terms of the effective Hamiltonian involving the ^{1}H-^{1}H dipolar interaction [38], pulse transients, rf inhomogeneites, and other experimental imperfections during the fixed $N{\cdot}t_R$ of the PM pulse and the total incremental $SR4_1^2$ recoupling periods (τ), giving the signal $S_0(\tau)$. Secondly, the identical experiment is run with the ^{14}N irradiation on PM pulse during $N{\cdot}t_R$ delay. This pulse prevents the refocusing of the ^{1}H-^{14}N heteronuclear dipolar coupling, while ^{1}H CSA is still refocused by the spin-echo. Hence, the achieved ^{1}H signal, $S'(\tau)$, is not only affected by the decaying effects as in the previous case but also modulated by the ^{1}H-^{14}N heteronuclear dipolar coupling. In the PM-S-RESPDOR fraction curve, the decaying effects are minimized by plotting $\Delta S/S_0 = (S_o(\tau) - S'(\tau))/S_o(\tau)$ as a function of mixing time, τ. Matching the experimental fraction curve with analytical/simulated curves enables the extraction of the dipolar coupling between ^{1}H and ^{14}N ($b_{1\text{H-}14\text{N}}/(2\pi)$); thus providing an accurate ^{1}H-^{14}N distance through the following equation:

$$^1\text{H-}\ ^{14}\text{N distance (Å)} = \left(\frac{120.1}{b_{1\text{H}-14\text{N}}/2\pi(\text{kHz})}\frac{\gamma_{14\text{N}}}{\gamma_{1\text{H}}}\right)^{1/3}, \quad (1)$$

where γ_X (X = ^{1}H or ^{14}N) represents the gyromagnetic ratio of the X nucleus and $b_{1\text{H-}14\text{N}}/(2\pi)$ is in kHz.

3. Numerical simulations

Numerical simulations were done using the SIMPSON package [39,40] with 232 (α_{CR}, β_{CR}) pairs according to the REPULSION algorithm [41] and 53 γ_{CR} angles, where the {α_{CR}, β_{CR}, γ_{CR}} Euler angles relate the crystal-fixed frame and the rotor-fixed frame. Simulations were performed on an isolated ^{1}H-^{14}N spin system at B_0 = 14.1 T. The isotropic and anisotropic chemical shifts of both ^{1}H and ^{14}N nuclei were disregarded. For ^{14}N nucleus, the quadrupolar interaction was considered up to second order, and the asymmetry parameter was set to zero. The orientations of ^{14}N quadrupolar interaction and ^{1}H-^{14}N dipolar interaction were characterized by the Euler angles (Ω_{PC}) of {0°, 0°, 0°} and {10°, 20°, 30°}, respectively, where P refers to the principal axis system while C refers to the crystal-fixecd frame. The delta function is assumed for the ^{1}H π pulse. Further details are given in the figure captions.

3.1. Feasibility at very fast MAS frequency

To test the feasibility of PM-S-RESPDOR at very fast MAS frequencies ($\nu_R \geq 70$ kHz), we performed simulations on a modeled ^{1}H-^{14}N spin system with $|b_{1\text{H-}14\text{N}}/(2\pi)|$ of 2.0 kHz under different MAS frequencies, varying from 20 kHz to 70 kHz. For objective comparisons, the PM pulse lengths for all simulations were set comparable to each other, ranging from 0.10 to 0.17 ms. We modeled an isolated system where only one ^{1}H spin is involved, meaning that there is no ^{1}H-^{1}H homonuclear dipolar interaction; hence, simulations can be tested even under moderate MAS frequencies. The analytical curve was derived from the Eq. (16) of ref. [25] under the assumption of complete saturation of ^{14}N (f = 1) and was also included for comparison:

$$\frac{\Delta S}{S_0} = \left\{\frac{2}{3} - \frac{\pi\sqrt{2}}{9}J_{1/4}\left(\frac{\pi}{4}(b_{1\text{H}-14\text{N}}/2\pi)\tau\right)J_{-1/4}\left(\frac{\pi}{4}(b_{1\text{H}-14\text{N}}/2\pi)\tau\right) - \frac{\pi\sqrt{2}}{18}J_{1/4}\left(\frac{\pi}{2}(b_{1\text{H}-14\text{N}}/2\pi)\tau\right)J_{-1/4}\left(\frac{\pi}{2}(b_{1\text{H}-14\text{N}}/2\pi)\tau\right)\right\} \quad (2)$$

where $J_{\pm 1/4}$ terms denote the ±1/4-order Bessel functions of the first kind. Under the ideal situation, the theoretical maximum of RESPDOR fraction curve is around $\Delta S/S_0 = 2I/(2I+1) \sim 0.67$ for spin number I = 1 as demonstrated by the analytical curve (unfilled circle) in Fig. 2. Moreover, in Fig. 2 it is observed that simulated fraction curves are almost identical to each other and are well reproduced by the analytical curve. These results confirm the feasibility of PM-S-RESPDOR at very fast MAS frequency. It is important that all the curves reach to the optimum $\Delta S/S_0$ at identical mixing time τ of ~1.6 ms, meaning that the RESPDOR fraction curves are still mainly governed by the first-order averaged Hamiltonian of the ^{1}H-^{14}N heteronuclear dipolar interaction. One point worth mentioning in Fig. 2 is the non-zero $\Delta S/S_0$ intensities even at τ = 0 ms, which can be possibly ascribed to the reintroduction of ^{1}H-^{14}N dipolar coupling during the PM pulse length. As the PM pulse is asymmetric with respect to its center, the reintroduced ^{1}H-^{14}N dipolar coupling during the PM pulse prevents the refocus of dephasing ^{1}H signals by the central ^{1}H π pulse, resulting in non-zero contribution to $\Delta S/S_0$ at τ = 0 ms. It is noted that the $\Delta S/S_0(\tau = 0)$ value gets larger with slower MAS frequency, namely among the simulated MAS frequencies (20–70 kHz), its intensity reaches maximum at 0.03 when MAS frequency is the slowest, at 20 kHz. Such behavior indicates the reintroduction of ^{1}H-^{14}N dipolar coupling comes not only from the first-order but also from the higher-order effects. The contribution of the higher-order terms is confirmed by the inverse proportion of $\Delta S/S_0(\tau = 0)$ intensity to MAS frequency, which can be largely suppressed under $\nu_R \geq 60$ kHz

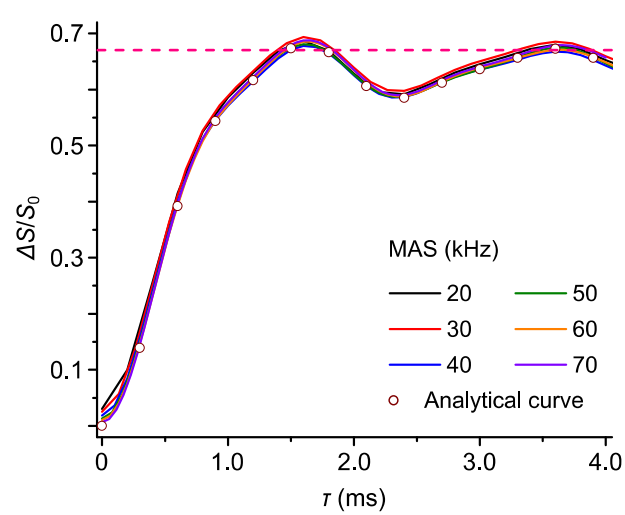

Fig. 2. Simulated PM-S-RESPDOR fraction curves (solid lines) where $\Delta S/S_0$ intensities were plotted as a function of τ for a powdered sample. An isolated ^{1}H-^{14}N spin system was used with $|b_{1\text{H-}14\text{N}}/(2\pi)|$ of 2.0 kHz and ^{14}N C_Q of 1.0 MHz. Simulations were performed at B_0 = 14.1 T and at different MAS frequencies ranging from 20 to 70 kHz. For objective comparisons among simulations, the PM pulse lengths were set from 0.10 to 0.17 ms while the $\nu_1(^{14}\text{N})$ was fixed at 83 kHz. The analytical curve (unfilled circle) was plotted with $|b_{1\text{H-}14\text{N}}/(2\pi)|$ of 2.0 kHz for comparison. The dash line represents the $\Delta S/S_0$ value of 0.67.

as shown in Fig. 2. This further necessitates the use of very fast MAS frequencies even for an isolated ^{1}H-^{14}N spin system when the fraction curve is fitted with the analytical RESPDOR curve. In short, the simulations not only verify the feasibility of PM-S-RESPDOR experiment at very fast MAS frequency but also show the advantage of fast MAS condition in minimizing the effect of high-order ^{1}H-^{14}N dipolar coupling terms introduced by the PM pulse. Hence, all the simulations below were performed under MAS frequency of 70 kHz.

3.2. Effects of ^{14}N radio-frequency field

The role of PM pulse is to saturate the polarizations of different ^{14}N energy levels, which is crucial for the performance of PM-S-RESPDOR. To investigate the effect of $\nu_1(^{14}\mathrm{N})$ on this saturation process, we performed simulations on an isolated ^{1}H-^{14}N spin system by varying $\nu_1(^{14}\mathrm{N})$ from 10 to 100 kHz with steps of 10 kHz. The ^{14}N C_Q was fixed at 4.0 MHz since this value is common for ^{14}N-containing organic molecules. Fig. 3 shows these simulated fraction curves under the PM pulse length of $10t_R$ and $|b_{1H\text{-}14N}/(2\pi)|$ of either 2.0 kHz (a) or 8.0 kHz (b). At first glance, all the simulated fraction curves reach their maximum at identical mixing time for a specific ^{1}H-^{14}N dipolar coupling, showing the main contribution of first-order $b_{1H\text{-}14N}/(2\pi)$ on dephasing process. For both Fig. 3a and b, the simulated curves with $\nu_1(^{14}\mathrm{N})$ of 80 kHz or larger are the best option since its maximum is the closet to $\Delta S/S_0$ of 0.67 and it oscillates around this value. It is noted that in Fig. 3b, the larger the $\nu_1(^{14}\mathrm{N})$, the further the $\Delta S/S_0(\tau = 0)$ deviates from 0. Such phenomenon, which was also observed in Fig. 2 at moderate and fast MAS frequency ($\nu_R \leq 60$ kHz), can be explained due to the reintroduction of ^{1}H-^{14}N dipolar coupling by the PM pulse. We also tested the effect of $\nu_1(^{14}\mathrm{N})$ with a PM pulse length of $46t_R$ (0.66 ms). However, such a long pulse makes the problem of non-zero $\Delta S/S_0(\tau = 0)$ more severe for large $|b_{1H\text{-}14N}/(2\pi)|$ (see Fig. S1), definitely affecting the accuracy of simulation fittings. This indicates that the non-zero $\Delta S/S_0(\tau = 0)$ is ascribed to the reintroduction of the ^{1}H-^{14}N dipolar coupling during the PM pulse. Overall, the PM pulse with $\nu_1(^{14}\mathrm{N})$ of 80 kHz and a length of $10t_R$ (0.14 ms) leads to (i) an efficient saturation of ^{14}N nucleus with C_Q of 4.0 MHz and (ii) an insignificant effect of recoupled ^{1}H-^{14}N dipolar interaction by the PM pulse. Next, the robustness of the PM pulse under these conditions with respect to different values of ^{14}N C_Q will be examined.

3.3. Robustness to ^{14}N quadrupolar interaction

For organic molecules, the ^{14}N C_Q can vary extensively. The strong quadrupolar interactions can significantly reduce the extent of saturation for ^{14}N nuclei, thus reducing the RESPDOR effect. Here, we investigate the robustness of PM pulse with $\nu_1(^{14}\mathrm{N})$ of 83 kHz and length of $10t_R$ (0.14 ms) with respect to ^{14}N quadrupolar interaction by simulations on an isolated ^{1}H-^{14}N spin system with $|b_{1H\text{-}14N}/(2\pi)|$ of 2.0 and 7.0 kHz while varying C_Q from 1.0 MHz to 6.0 MHz. The analytical curve was also plotted for comparison in the case $|b_{1H\text{-}14N}/(2\pi)|$ of 2.0 kHz. The results, shown in Fig. 4a and b for $|b_{1H\text{-}14N}/(2\pi)|$ of 2.0 and 7.0 kHz, respectively, reveal that all simulated fraction curves slightly deviate from each other; however, they all reach their corresponding maximum $\Delta S/S_0$ at identical τ value. This again verifies the main contribution of the first-order ^{1}H-^{14}N dipolar coupling in the fraction curves. For $|b_{1H\text{-}14N}/(2\pi)|$ of 2.0 kHz, the simulated curves with C_Q from 1.0 to 4.0 MHz well match with the analytical curve while those with larger C_Q values slightly differ. This situation is also observed for strong $|b_{1H\text{-}14N}/(2\pi)|$ of 7.0 kHz, where the maxima from the simulated fraction curves with C_Q of 5.0 and 6.0 MHz are under the $\Delta S/S_0$ value of 0.67. Nevertheless, such deviations are not significant, indicating a high robustness of PM pulse with respect to ^{14}N quadrupolar interaction under MAS frequency of 70 kHz. We also performed the same simulations with PM pulse length of $46t_R$, shown in Fig. S2. While Fig. S2a shows the similar picture with Fig. 4a, simulations in Fig. S2b show poorer robustness to different C_Q values than those in Fig. 4b. Not only less robustness to ^{14}N C_Q, an additional disadvantage of using long PM pulse length is the problem of non-zero $\Delta S/S_0(\tau = 0)$ due to the reintroduction of ^{1}H-^{14}N dipolar coupling by the PM pulse, as mentioned in the previous section. In Fig. 4a, $\Delta S/S_0(\tau = 0)$ intensities for varying C_Q are almost 0 while in Fig. S2a, they are not and get larger at smaller C_Q values. This shows that the recoupling efficiency of ^{1}H-^{14}N dipolar coupling is proportional to the PM pulse length but inversely proportional to C_Q values. Furthermore, comparing Fig. 4a and b, the non-zero $\Delta S/S_0(\tau = 0)$ for $|b_{1H\text{-}14N}/(2\pi)|$ of 7.0 kHz but not for 2.0 kHz indicates that the reintroduction of ^{1}H-^{14}N dipolar coupling is better at larger size of $b_{1H\text{-}14N}/(2\pi)$. We can briefly conclude that the recoupling efficiency of ^{1}H-^{14}N dipolar coupling is proportional to the PM pulse length, $b_{1H\text{-}14N}/(2\pi)$, and $\nu_1(^{14}\mathrm{N})$ while inversely proportional to C_Q and MAS frequency. The detailed analysis of the reintroduced ^{1}H-^{14}N dipolar coupling by PM pulse is out of the scope of this work, thus the investigation was not performed. For the sake of simplicity, the $\Delta S/S_0(\tau = 0)$ intensity should be as small as possible, while at the same time the experimental parameters should ensure the strong robustness to varying C_Q and/or $b_{1H\text{-}14N}/(2\pi)$ values. Based on all the simulations, the PM pulse with a length of $10t_R$ and a ^{14}N rf field of 83 kHz meets all the requirements; hence these conditions will be employed for the following experiments. This is an important result since we still can fit the

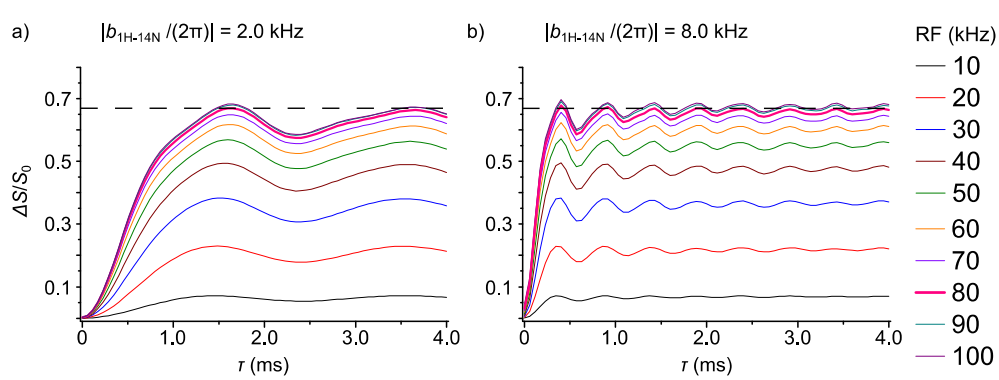

Fig. 3. Simulated PM-S-RESPDOR fraction curves where $\Delta S/S_0$ intensities were plotted as a function of τ for a powdered sample. An isolated ^{1}H-^{14}N spin system was defined as follows: $|b_{1H\text{-}14N}/(2\pi)|$ was 2.0 kHz (a) and 8.0 kHz (b) while the ^{14}N C_Q value was fixed at 4.0 MHz. Simulations were performed at $B_0 = 14.1$ T and $\nu_R = 70$ kHz. The PM pulse length was $10t_R$ (0.14 ms) while $\nu_1(^{14}\mathrm{N})$ was varied from 10 to 100 kHz with steps of 10 kHz. The dash line represents the $\Delta S/S_0$ value of 0.67.

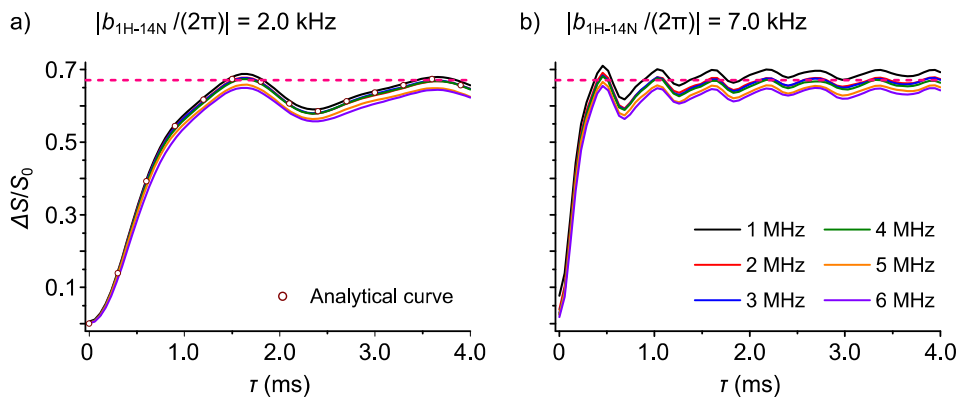

Fig. 4. Simulated PM-S-RESPDOR fraction curves (solid lines) where $\Delta S/S_0$ intensities were plotted as a function of τ for a powdered sample. An isolated ^{1}H-^{14}N spin system was defined as follows: $|b_{1H\text{-}14N}/(2\pi)|$ was 2.0 kHz (a) and 7.0 kHz (b) while the ^{14}N C_Q values were varied from 1.0 MHz to 6.0 MHz. Simulations were performed at B_0 = 14.1 T and ν_R = 70 kHz. The PM pulse length and ν_1 were $10t_R$ (0.14 ms) and 83 kHz, respectively. The analytical curve (unfilled circle) was also included for comparison in (a). The dash line represents the $\Delta S/S_0$ value of 0.67.

experimental fraction curves without a prior knowledge on a system of interest, or in other words, the analytical expression can be used for extracting distances.

4. Materials and methods

L-tyrosine·HCl (Tyr) and N-acetyl-L-alanine (Ac-Ala) were purchased form Sigma-Aldrich and used as received. The samples were separately packed into 1 mm zirconia rotors and then inserted into 1 mm ^{1}H/X double-resonance probe. The rotors were spun at a MAS frequency of 70 kHz. All NMR experiments were recorded at a room temperature of 25 °C on JNM-ECZ600R (JEOL RESONANCE Inc.) at 14.1 T solid-state NMR spectrometers. The ^{1}H and ^{14}N Larmor frequencies are 600.0 and 43.4 MHz, respectively. The ^{1}H and ^{14}N shifts have been referenced so that the ^{14}N resonance of NH_4Cl is −337 ppm while the ^{1}H resonance of uniformly ^{13}C-^{15}N labeled L-alanine is 1.5 ppm. The ^{1}H rf-field was 217 kHz for $\pi/2$ and π pulses and 140 kHz for the $SR4_1^2$ sequence. For *D*-HMQC experiments, the ^{14}N pulse lengths and $\nu_1(^{14}N)$ were 5 μs and 83 kHz, respectively, and ^{14}N SQ coherence was selected during the t_1 evolution. For PM-S-RESPDOR experiments, the length of the PM pulse was $10t_R$ (0.14 ms) and $\nu_1(^{14}N)$ was 83 kHz for both samples. The ^{14}N rf-field was calibrated by NH_4Cl. The two-dimensional (2D) ^{1}H-{^{14}N} *D*-HMQC spectrum of Tyr was recorded using the sequence shown in Fig. 1a with 24 scans, 72 t_1 points, and rotor-synchronized t_1 increment of 14.3 μs. The τ and recycling delay were 400 μs and 3.5 s, respectively. The total experimental time was 3.4 h. The States-TPPI method was employed for the quadrature detection along the indirect dimension. The PM-S-RESPDOR fraction curves were recorded using the sequence shown in Fig. 1b. Prior to measurements, 64 dummy scans were applied for both Tyr and Ac-Ala in order to reach the steady state. The τ value was varied from ~0.1 to 2.0 ms for Tyr and from 0 to 1.7 ms for Ac-Ala, both with a step of 57.1 μs. The number of scans and recycle delays were (32, 9.0 s) and (64, 18.0 s) for Tyr and Ac-Ala, respectively. These fraction curves took about 6 h for Tyr and 20 h for Ac-Ala.

5. Experimental demonstration

5.1. L-tyrosine·HCl

The chemical structure of Tyr is shown as an inset in Fig. 5. It only consists of one ^{14}N site, which belongs to the NH_3^+ group; hence, the magnitude of C_Q is small (approximately 1.0 MHz)

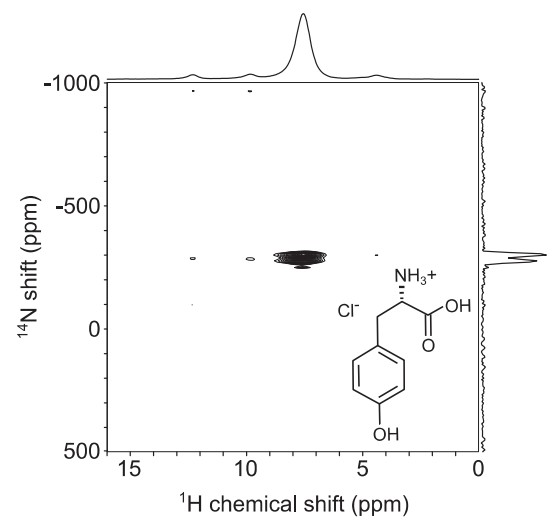

Fig. 5. 2D ^{1}H-{^{14}N} *D*-HMQC spectrum of Tyr (inset) with ^{1}H-^{14}N correlations. The experiment was run with 24 scans, 72 t_1 points, and rotor-synchronized t_1 increment of 14.3 μs. The τ and recycle delay were 400 μs and 3.5 s, respectively. The experimental time was ~3.4 h.

owing to its symmetric surrounding environment [42]. Fig. 5 shows a (^{1}H, ^{14}N) correlation at 7.7 ppm and −290.0 ppm, respectively, we thus can unambiguously assign the ^{1}H at 7.7 ppm to three protons of NH_3^+ group. Other correlations between different ^{1}H sites, e.g. at 4.5 ppm attributed to the CH_2 protons, and the single ^{14}N site are also observed but their intensities are much weaker. This is due to their longer distances to the ^{14}N site compared to ^{1}H resonance at 7.7 ppm, requiring longer τ for sufficient sensitivities.

Fig. 6 shows the results for the distance measurements in Tyr using the PM-S-REPSPDOR technique. The errors (or uncertainties) of $\Delta S/S_0$ intensities are calculated based on the signal-to-noise ratios of S' and S_0 signals and displayed as the vertical bars in Fig. 6. The extraction of $b_{1H\text{-}14N}/(2\pi)$ value is based on the best fitting of experimental $\Delta S/S_0$ fraction curves with the analytical ones using Eq. (2). The values that have root mean square deviation (RMSD) about two times of the smallest RMSD are selected and these values are used for calculating the averaged ^{1}H-^{14}N distance and its standard deviation according to Eq. (1). In Fig. 6a, the fraction curve at ^{1}H chemical shift of 7.7 ppm reaches its maximum $\Delta S/S_0$ intensity at τ of ~1.4 ms, and then the signal drops down.

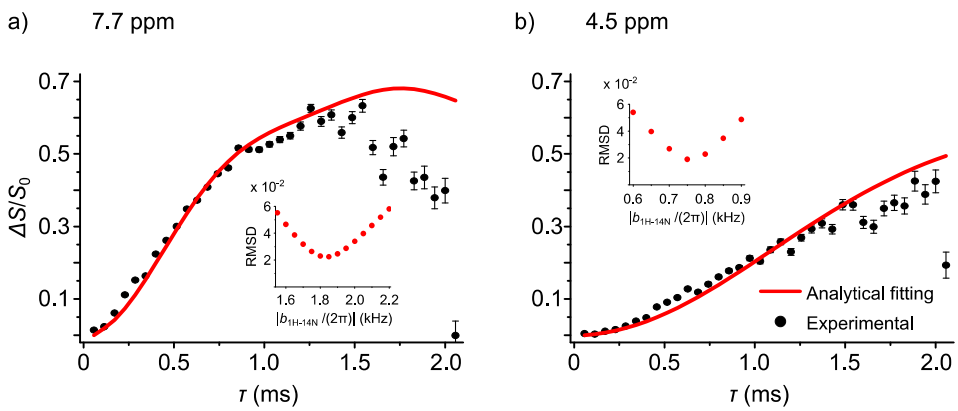

Fig. 6. Tyr: the experimental ^{1}H-^{14}N fraction curves at ^{1}H chemical shift of 7.7 ppm (a) and 4.5 ppm (b) achieved by PM-S-RESPDOR (dots) and the fitting curves by the analytical expression (solid lines). The errors of $\Delta S/S_0$ intensities are displayed as the vertical bars. The experimental time was ~6 h. The insets show the best fitting ^{1}H-^{14}N dipolar coupling values based on the RMSD analysis. Fittings are performed solely by adjusting $b_{1H\text{-}14N}/(2\pi)$ in Eq. (2) without any scaling of $\Delta S/S_0$ dataset.

The large fluctuation of $\Delta S/S_0$ at $\tau > 1.4$ ms is attributed to poor signal-to-noise ratio of both S' and S_0, making the $\Delta S/S_0$ unreliable. Hence, for accurate extraction of $b_{1H\text{-}14N}/(2\pi)$, the points at $\tau > 1.4$ ms are neglected. The fraction curve is well fitted with the analytical curve up to $\tau \sim 1.4$ ms, achieving a ^{1}H-^{14}N distance of 1.68 Å ± 0.04 Å without any vertical scaling. Such distance is much longer than the directly bonded H-N distance, which is approximately 1.0 Å. It indicates that the $b_{1H\text{-}14N}/(2\pi)$ is dynamically averaged, resulting from the fast rotation of the three protons (NH_3 group) along the C-N bond direction. The dynamically averaged $b_{1H\text{-}14N}/(2\pi)$ can be related to the original $b_{1H\text{-}14N}/(2\pi)$ with a modulation factor $P_2(\cos(\Theta))$ (Θ denotes the angle between H-N and C-N of 109.5°):

$$(\text{Original } b_{1H-14N}/(2\pi)) \times |P_2(\cos(109.5^\circ)| = (\text{Averaged } b_{1H-14N}/(2\pi)), \quad (3)$$

or in terms of distance:

$$(\text{Original H} - \text{N distance}) = (\text{Averaged H} - \text{N distance}) \times |P_2(\cos(109.5^\circ))^{1/3}|. \quad (4)$$

Therefore, the original H-N distance can be calculated as 1.68 Å × $|P_2(\cos\ 109.5^\circ)^{1/3}|$ = 1.16 Å, agreeing well with the H-N distance of 1.01 Å, determined by neutron diffraction technique (CSD entry: LTYRHC10) [43]. The longer distance in PM-S-RESPDOR than those measured by neutron data may be ascribed to the different vibrational averages of the internuclear distances in ssNMR and diffraction [44]. These reasons make the distances derived from diffraction measurements always shorter than the actual values especially for short distances (typically several percent shorter) [45]. Lower $\Delta S/S_0$ intensity in the fraction curve at ^{1}H chemical shift of 4.5 ppm (Fig. 6b) is observed compared to that at ^{1}H chemical shift of 7.7 ppm (Fig. 6a), indicating a slower dephasing rate or in other words a further distance to the ^{14}N site. This is consistent with the qualitative observation from *D*-HMQC experiment shown in Fig. 5. It is worth noting that both fraction curves in Fig. 6a and b exhibit similar error bars, hence the fitting was also processed up to $\tau \sim 1.4$ ms. The best fitting is obtained with a ^{1}H-^{14}N distance of 2.24 Å ± 0.07 Å, in good agreement with neutron diffraction H-N distance of 2.10 Å (CSD entry: LTYRHC10) [43]. It should be again emphasized that the fitting by the analytical expression was performed only with varying the dipolar interactions without any vertical scaling. In short, these results prove the simplicity and accuracy of the PM-S-RESPDOR for multiple ^{1}H-^{14}N distance measurements.

5.2. N-acetyl-L-alanine

To investigate the feasibility of PM-S-RESPDOR for samples with larger ^{14}N C_Q values, experiments have been performed on Ac-Ala, whose structure is shown in the middle panel of Fig. 7. The quadrupolar product is estimated to be 3.4 MHz from the difference between ^{14}N and ^{15}N shifts, which is consistent with that frequently observed in the amide nitrogen. While large uncertainties of $\Delta S/S_0$ intensities at long τ are observed for the fraction curve at ^{1}H of 7.9 ppm in Fig. 7a, the fraction curve at ^{1}H of 3.9 ppm in Fig. 7b exhibit almost no errors. From the fitting of the analytical curves (solid line) to the experimental ones (dots) in Fig. 7a and b, the ^{1}H-^{14}N distances at (^{1}H: 7.9 ppm (NH site), ^{14}N: 200 ppm) and (^{1}H: 3.9 ppm (CH site), ^{14}N: 200 ppm) were calculated to be 1.06 Å ± 0.02 Å and 2.11 Å ± 0.05 Å, respectively. It is noted that the fitting of the fraction curve at ^{1}H of 7.9 ppm was performed by using τ only up to 0.4 ms while that at ^{1}H of 3.9 ppm was up to 1.7 ms. Such difference in fitting will be explained later. While the latter agrees well with the distance of 2.09 Å from single crystal X-ray diffraction, the former is longer than the reported N-H bond length of 0.78 Å (CSD entry: ATUVIU) [46]. This is because the X-ray method approximates the center of electron density but not the atomic position, and it is poor at locating the hydrogen position due to a limited scattering power of hydrogen in addition to the vibrational effect discussed above. Another advantage of our method is that measurements can be done at room temperature (298 K) while it was at low temperature (105 K) for X-ray study [46]. In conclusion, even for a difficult system where the $b_{1H\text{-}14N}/(2\pi)$ is strong and ^{14}N C_Q value is large, the PM-S-RESPDOR sequence is applicable for providing multiple accurate ^{1}H-^{14}N distances in a single experiment.

One important point to mention is that we repeatedly observe a good fitting until the first oscillation appears while the random noise behavior appears beyond that point. We speculate that this is because of the combined effects of spinning fluctuation and size of ^{1}H-^{14}N dipolar couplings. The spinning fluctuation introduces noise as observed in *D*-HMQC experiments. As mentioned before, two SR4 blocks should be rotor-synchronized, otherwise the reintroduced ^{1}H-^{14}N dipolar prevents the echo formation of ^{1}H signals. Thus, random fluctuation of sample spinning introduces random variation of ^{1}H PM-S-RESPDOR signals. The extent of variation depends on the degree of spinning fluctuation as well as on the size of ^{1}H-^{14}N dipolar interactions. While the former is the same for all the spins, the latter depends on spin pairs. When ^{1}H-^{14}N dipolar coupling is small, the effect of spinning fluctuation is insignificant because of the small recoupled interaction, allowing the formation

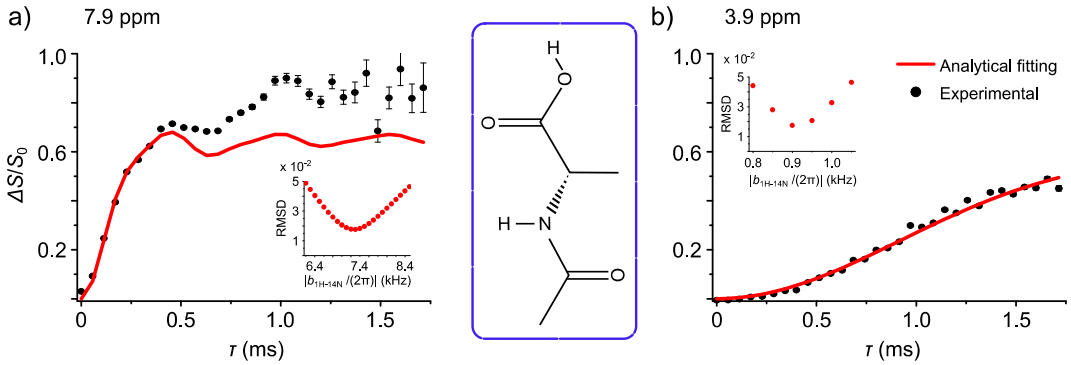

Fig. 7. Ac-Ala: the experimental ^{1}H-^{14}N fraction curves at ^{1}H chemical shift of 7.9 ppm (a) and 3.9 ppm (b) achieved by PM-S-RESPDOR (dots) and the fitting curves by the analytical expression (solid lines). The errors of $\Delta S/S_0$ intensities are displayed as the vertical bars. The structure of Ac-Ala is shown in the middle of Figs. a and b, where ^{1}H chemical shifts of 7.9 ppm and 3.9 ppm correspond to N**H** and C**H** sites, respectively. The experimental time was ~20 h. The insets show the best fitting ^{1}H-^{14}N dipolar coupling values based on RMSD analysis. Fittings are performed solely by adjusting $b_{1H\text{-}14N}/(2\pi)$ using Eq. (2) without any scaling of $\Delta S/S_0$ dataset.

of an echo even with long recoupling times (τ). On the other hand, the effect of spinning fluctuation is amplified for strongly coupled ^{1}H-^{14}N pairs due to the large recoupled interaction, hampering the formation of an echo for long recoupling times. We have performed preliminary investigation by introducing small delays before the first and after the second SR4 blocks mimicking the spinning fluctuation. A larger deviation is observed in the stronger coupled ^{1}H-^{14}N pair, qualitatively agreeing with the experimental observation (Fig S3). This also explains for experimental observations; the fitting of the fraction curve for stronger couplings of ^{1}H at 7.9 ppm of Ac-Ala was only up to 0.4 ms while for weaker coupling they were up to 1.4 ms for ^{1}H of L-tyrosine and 1.7 ms for ^{1}H at 3.9 ppm of Ac-Ala. We are now investigating the phenomena of large deviations of strong ^{1}H-^{14}N dipolar coupling in the presence of spinning fluctuation in detail and the results will be published elsewhere. It is worth examining the effect of the second-nearest ^{14}N neighbor on the $\Delta S/S_0$ fraction curves since hitherto our analysis is only based on an isolated ^{1}H-^{14}N system. We have performed simulations on a two-spin and three-spin systems based on the XRD structure of Ac-Ala. For the former, it consists of an isolated ^{1}H-^{14}N system while for the latter, an addition of the second-nearest ^{14}N nucleus is involved. As shown in Fig. S4, the $\Delta S/S_0$ fraction curves of the two-spin (black) and three-spin system (red) are similar under the $|b_{1H\text{-}14N}/(2\pi)|$ of 7.0 (a) and 1.0 (b) kHz. The effect of the second ^{14}N nucleus is less significant even for smaller dipolar couplings (Fig. S4(b)). In short, under our working conditions, the effect of the second-nearest ^{14}N neighbor to an isolated ^{1}H-^{14}N system is insignificant, or in other words the assumption of an isolated ^{1}H-^{14}N system for analytical curve fitting is still valid.

6. Conclusion

In this work, we have managed to use the combination of a phase-modulated pulse and the S-RESPDOR sequence (PM-S-RESPDOR) for the measurement of ^{1}H-^{14}N distances at very fast MAS frequency. Numerical spin dynamics simulations have shown the high robustness of the PM pulse with respect to large variations of dipolar couplings and quadrupolar coupling constants with $\nu_1(^{14}\text{N})$ of 80 kHz and more, and a length of $10t_R$. Such advances have enabled a simple fitting procedure without vertical scaling by just adjusting the ^{1}H-^{14}N dipolar coupling strengths using an analytical equation for matching with experimental fraction curves. Another important point for the PM-S-RESPDOR sequence is the ability to measure multiple distances since the dipolar truncation effect is avoided. The experimental verifications were subsequently performed on L-tyrosine·HCl and N-acetyl-L-alanine samples. The obtained ^{1}H-^{14}N distances are consistent with those derived from diffraction techniques. With simple implementation and accurate distance measurements, we believe that this new PM-S-RESPDOR sequence can be useful on other systems and on other quadrupolar nuclei.

Acknowledgement

This work was supported by JSPS KAKENHI Grant numbers JP17H03043. AG & MM are supported by BSF grant #2016169, F.R. thanks Jeol (Italia) S.p.A. for a Ph.D. scholarship.

Appendix A. Supplementary material

Supplementary data to this article can be found online at https://doi.org/10.1016/j.jmr.2019.07.046.

References

[1] C.M. Rienstra, L. Tucker-Kellogg, C.P. Jaroniec, M. Hohwy, B. Reif, M.T. McMahon, B. Tidor, T. Lozano-Perez, R.G. Griffin, De novo determination of peptide structure with solid-state magic-angle spinning NMR spectroscopy, Proc. Natl. Acad. Sci. 99 (2002) 10260–10265, https://doi.org/10.1073/pnas.152346599.

[2] W.T. Franks, B.J. Wylie, H.L.F. Schmidt, A.J. Nieuwkoop, R.-M. Mayrhofer, G.J. Shah, D.T. Graesser, C.M. Rienstra, Dipole tensor-based atomic-resolution structure determination of a nanocrystalline protein by solid-state NMR, Proc. Natl. Acad. Sci. 105 (2008) 4621–4626, https://doi.org/10.1073/pnas.0712393105.

[3] L. Rajput, M. Banik, J.R. Yarava, S. Joseph, M.K. Pandey, Y. Nishiyama, G.R. Desiraju, Exploring the salt-cocrystal continuum with solid-state NMR using natural-abundance samples: implications for crystal engineering, IUCrJ. 4 (2017) 466–475, https://doi.org/10.1107/S205225251700687X.

[4] E.R.R. Andrew, A. Bradbury, R.G.G. Eades, Nuclear magnetic resonance spectra from a crystal rotated at high speed 1659 1659 Nature 182 (1958), https://doi.org/10.1038/1821659a0.

[5] S. Dusold, A. Sebald, Dipolar recoupling under magic-angle spinning conditions, Annu. Rep. NMR Spectrosc. (2000) 185–264, https://doi.org/10.1016/S0066-4103(00)41010-0.

[6] G. De Paëpe, Dipolar recoupling in magic angle spinning solid-state nuclear magnetic resonance, Annu. Rev. Phys. Chem. 63 (2012) 661–684, https://doi.org/10.1146/annurev-physchem-032511-143726.

[7] M. Hohwy, C.P. Jaroniec, B. Reif, C.M. Rienstra, R.G. Griffin, Local structure and relaxation in solid-state NMR: accurate measurement of amide N–H bond lengths and H–N–H bond angles, J. Am. Chem. Soc. 122 (2000) 3218–3219, https://doi.org/10.1021/ja9913737.

[8] B.J. Van Rossum, C.P. De Groot, V. Ladizhansky, S. Vega, H.J.M. De Groot, A method for measuring heteronuclear (1H–13C) distances in high speed MAS NMR, J. Am. Chem. Soc. 122 (2000) 3465–3472, https://doi.org/10.1021/ja992714j.

[9] I. Schnell, K. Saalwächter, ^{15}N–^{1}H bond length determination in natural abundance by inverse detection in fast-MAS solid-state NMR spectroscopy, J. Am. Chem. Soc. 124 (2002) 10938–10939, https://doi.org/10.1021/ja026657x.

[10] R. Fu, Measurement of ^{15}N–^{1}H bond lengths by rotational-echo double-resonance NMR spectroscopy, Chem. Phys. Lett. 376 (2003) 62–67, https://doi.org/10.1016/S0009-2614(03)00951-5.
[11] V. Chevelkov, U. Fink, B. Reif, Accurate determination of order parameters from ^{1}H, ^{15}N dipolar couplings in MAS solid-state NMR experiments, J. Am. Chem. Soc. 131 (2009) 14018–14022, https://doi.org/10.1021/ja902649u.
[12] P. Schanda, B.H. Meier, M. Ernst, Accurate measurement of one-bond H-X heteronuclear dipolar couplings in MAS solid-state NMR, J. Magn. Reson. 210 (2011) 246–259, https://doi.org/10.1016/j.jmr.2011.03.015.
[13] X. Zhao, J.L. Sudmeier, W.W. Bachovchin, M.H. Levitt, Measurement of NH bond lengths by fast magic-angle spinning solid-state NMR spectroscopy: a new method for the quantification of hydrogen bonds, J. Am. Chem. Soc. 123 (2001) 11097–11098, https://doi.org/10.1021/ja016328p.
[14] M.H. Levitt, Symmetry-based pulse sequences in magic-angle spinning solid-state NMR, in: Encyclopedia of Magnetic Resonance, John Wiley & Sons, Ltd, Chichester, UK, 2007, pp. 351–364. doi:10.1002/9780470034590.emrstm0551.
[15] G. Hou, I.J.L. Byeon, J. Ahn, A.M. Gronenborn, T. Polenova, ^{1}H–^{13}C/^{1}H-^{15}N heteronuclear dipolar recoupling by R-symmetry sequences under fast magic angle spinning for dynamics analysis of biological and organic solids, J. Am. Chem. Soc. 133 (2011) 18646–18655, https://doi.org/10.1021/ja203771a.
[16] G. Hou, X. Lu, A.J. Vega, T. Polenova, Accurate measurement of heteronuclear dipolar couplings by phase-alternating R-symmetry (PARS) sequences in magic angle spinning NMR spectroscopy, J. Chem. Phys. 141 (2014), https://doi.org/10.1063/1.4894226.
[17] X. Lu, H. Zhang, M. Lu, A.J. Vega, G. Hou, T. Polenova, Improving dipolar recoupling for site-specific structural and dynamics studies in biosolids NMR: windowed RN-symmetry sequences, Phys. Chem. Chem. Phys. 18 (2016) 1–10, https://doi.org/10.1039/C5CP07818K.
[18] P. Paluch, T. Pawlak, J.P. Amoureux, M.J. Potrzebowski, Simple and accurate determination of X-H distances under ultra-fast MAS NMR, J. Magn. Reson. 233 (2013) 56–63, https://doi.org/10.1016/j.jmr.2013.05.005.
[19] Y. Nishiyama, M. Malon, M.J. Potrzebowski, P. Paluch, J.P. Amoureux, Accurate NMR determination of C-H distances for unlabeled small molecules, Solid State Nucl. Magn. Reson. 73 (2015) 1–7, https://doi.org/10.1016/j.ssnmr.2015.06.005.
[20] A. Naito, A. Root, C.A. McDowell, Combined sample rotation and multiple-pulse NMR spectroscopic studies on protons bonded to nitrogen-14 nuclei in solid amino acids, J. Phys. Chem. 95 (1991) 3578–3581, https://doi.org/10.1021/j100162a027.
[21] Z. Gan, Measuring multiple carbon-nitrogen distances in natural abundant solids using R-RESPDOR NMR, Chem. Commun. (2006) 4712–4714, https://doi.org/10.1039/b611447d.
[22] T.G. Oas, R.G. Griffin, M.H. Levitt, Rotary resonance recoupling of dipolar interactions in solid-state nuclear magnetic resonance spectroscopy, J. Chem. Phys. 89 (1988) 692–695, https://doi.org/10.1063/1.455191.
[23] A. Brinkmann, A.P.M. Kentgens, Proton-selective O-17-H-1 distance measurements in fast magic-angle-spinning solid-state NMR spectroscopy for the determination of hydrogen bond lengths, J. Am. Chem. Soc. 128 (2006) 14758–14759, https://doi.org/10.1021/ja065415k.
[24] L. Chen, X. Lu, Q. Wang, O. Lafon, J. Trébosc, F. Deng, J.P. Amoureux, Distance measurement between a spin-1/2 and a half-integer quadrupolar nuclei by solid-state NMR using exact analytical expressions, J. Magn. Reson. 206 (2010) 269–273, https://doi.org/10.1016/j.jmr.2010.07.009.
[25] L. Chen, Q. Wang, B. Hu, O. Lafon, J. Trébosc, F. Deng, J.P. Amoureux, Measurement of hetero-nuclear distances using a symmetry-based pulse sequence in solid-state NMR, Phys. Chem. Chem. Phys. 12 (2010) 9395–9405, https://doi.org/10.1039/b926546e.
[26] X. Lu, O. Lafon, J. Trébosc, J.P. Amoureux, Detailed analysis of the S-RESPDOR solid-state NMR method for inter-nuclear distance measurement between spin-1/2 and quadrupolar nuclei, J. Magn. Reson. 215 (2011) 34–49, https://doi.org/10.1016/j.jmr.2011.12.009.
[27] F. Pourpoint, J. Trébosc, R.M. Gauvin, Q. Wang, O. Lafon, F. Deng, J.P. Amoureux, Measurement of aluminum-carbon distances using S-RESPDOR NMR experiments, ChemPhysChem 13 (2012) 3605–3615, https://doi.org/10.1002/cphc.201200490.
[28] T. Gullion, J. Schaefer, Rotational-echo double-resonance NMR, J. Magn. Reson. 81 (1989) (1969) 196–200, https://doi.org/10.1016/0022-2364(89)90280-1.
[29] E. Nimerovsky, R. Gupta, J. Yehl, M. Li, T. Polenova, A. Goldbourt, Phase-modulated LA-REDOR: A robust, accurate and efficient solid-state NMR technique for distance measurements between a spin-1/2 and a quadrupole spin, J. Magn. Reson. 244 (2014) 107–113, https://doi.org/10.1016/j.jmr.2014.03.003.
[30] E. Nimerovsky, M. Makrinich, A. Goldbourt, Analysis of large-anisotropy-spin recoupling pulses for distance measurement under magic-angle spinning NMR shows the superiority and robustness of a phase modulated saturation pulse, J. Chem. Phys. 146 (2017), https://doi.org/10.1063/1.4978472.
[31] M. Makrinich, R. Gupta, T. Polenova, A. Goldbourt, Saturation capability of short phase modulated pulses facilitates the measurement of longitudinal relaxation times of quadrupolar nuclei, Solid State Nucl. Magn. Reson. 84 (2017) 196–203, https://doi.org/10.1016/j.ssnmr.2017.04.003.
[32] M. Makrinich, E. Nimerovsky, A. Goldbourt, Pushing the limit of NMR-based distance measurements – retrieving dipolar couplings to spins with extensively large quadrupolar frequencies, Solid State Nucl. Magn. Reson. 92 (2018) 19–24, https://doi.org/10.1016/j.ssnmr.2018.04.001.
[33] Z. Gan, J.P. Amoureux, J. Trébosc, Proton-detected 14N MAS NMR using homonuclear decoupled rotary resonance, Chem. Phys. Lett. 435 (2007) 163–169, https://doi.org/10.1016/j.cplett.2006.12.066.
[34] S. Cavadini, A. Abraham, G. Bodenhausen, Proton-detected nitrogen-14 NMR by recoupling of heteronuclear dipolar interactions using symmetry-based sequences, Chem. Phys. Lett. 445 (2007) 1–5, https://doi.org/10.1016/j.cplett.2007.07.060.
[35] Y. Nishiyama, Y. Endo, T. Nemoto, H. Utsumi, K. Yamauchi, K. Hioka, T. Asakura, Very fast magic angle spinning (1)H-(14)N 2D solid-state NMR: sub-micro-liter sample data collection in a few minutes, J. Magn. Reson. (San Diego, Calif.: 1997) 208 (2011) 44–48, https://doi.org/10.1016/j.jmr.2010.10.001.
[36] G. Tricot, J. Trébosc, F. Pourpoint, R. Gauvin, L. Delevoye, The D-HMQC MAS-NMR technique, in: Annual Reports on NMR Spectroscopy, first ed., Elsevier Ltd., 2014, pp. 145–184. doi:10.1016/B978-0-12-800185-1.00004-8.
[37] N.C. Nielsen, H. Bildsøe, H.J. Jakobsen, M.H. Levitt, Double-quantum homonuclear rotary resonance: efficient dipolar recovery in magic-angle spinning nuclear magnetic resonance, J. Chem. Phys. 101 (1994) 1805–1812, https://doi.org/10.1063/1.467759.
[38] C. Filip, M. Bertmer, D.E. Demco, B. Blümich, Application of the floquet theory to multiple quantum NMR of dipolar-coupled multi-spin systems under magic angle spinning, Mol. Phys. 99 (2001) 1575–1587, https://doi.org/10.1080/00268970110060118.
[39] M. Bak, J.T. Rasmussen, N.C. Nielsen, SIMPSON: a general simulation program for solid-state NMR spectroscopy, J. Magn. Reson. (San Diego, Calif.: 1997) 147 (2000) 296–330, https://doi.org/10.1016/j.jmr.2011.09.008.
[40] Z. Tošner, R. Andersen, B. Stevensson, M. Edén, N.C. Nielsen, T. Vosegaard, Computer-intensive simulation of solid-state NMR experiments using {SIMPSON}, J. Magn. Reson. 246 (2014) 79–93, https://doi.org/10.1016/j.jmr.2014.07.002.
[41] M. Bak, N.C. Nielsen, Repulsion a novel approach to efficient powder averaging in solid-state NMR, J. Magn. Reson. 125 (1997) 132–139, https://doi.org/10.1006/jmre.1996.1087.
[42] D.T. Edmonds, C.P. Summers, ^{14}N pure quadrupole resonance in solid amino acids, J. Magn. Reson. 12 (1973) (1969) 134–142, https://doi.org/10.1016/0022-2364(73)90136-4.
[43] M.N. Frey, T.F. Koetzle, M.S. Lehmann, W.C. Hamilton, Precision neutron diffraction structure determination of protein and nucleic acid components. X. A comparison between the crystal and molecular structures of L-tyrosine and L-tyrosine hydrochloride, J. Chem. Phys. 58 (1973) 2547–2556, https://doi.org/10.1063/1.1679537.
[44] Y. Ishii, T. Terao, S. Hayashi, Theory and simulation of vibrational effects on structural measurements by solid-state nuclear magnetic resonance, J. Chem. Phys. 107 (1997) 2760–2774, https://doi.org/10.1063/1.474633.
[45] M. Fugel, D. Jayatilaka, E. Hupf, J. Overgaard, V.R. Hathwar, P. Macchi, M.J. Turner, J.A.K. Howard, O.V. Dolomanov, H. Puschmann, B.B. Iversen, H.B. Bürgi, S. Grabowsky, Probing the accuracy and precision of Hirshfeld atom refinement with HARt interfaced with Olex 2, IUCrJ. 5 (2018) 32–44, https://doi.org/10.1107/S2052252517015548.
[46] C.H. Görbitz, E. Sagstuen, N-acetyl-L-alanine, Acta Crystallogr. Sect. E Struct. Rep. Online 60 (2004) o860–o862. doi:10.1107/S1600536804009353.